Eurasian Journal of Analytical Chemistry
ISSN: 1306-3057 OPEN ACCESS 2017 12 (4): 224-234

Texture Classification based on DLBP

K. Anita Davamani*, S. Amudha

Received: 10 December 2016 ▪ Revised: 13 January 2017 ▪ Accepted: 12 February 2017

Abstract: The uniqueness of a fingerprint can be determined by the pattern of ridges and furrows as well as the minutiae points. Minutia consists of short ridges, Ridge ending and Bifurcation. Fingerprint representations are based on the entire image, finger ridges, pores on the ridges, or salient features derived from the ridges. Representations predominantly based on ridge endings or bifurcations collectively known as minutiae. The paper proposes a novel approach to extract image features for Fingerprint texture classification. It makes use of the features extracted using Dominant local binary patterns (DLBP). The dominant local binary pattern method makes use of the most frequently occurred patterns to capture descriptive textural information, while the Gabor-based features aim at supplying additional global textural information to the DLBP features. These features are classified using Support Vector Machine (SVM) classifier. It is experimentally demonstrated that the proposed method achieves the highest classification accuracy in various texture databases and image conditions.

Keywords: Bactericidal, Disk Diffusion, Microalgae, Antibiotics, Pathogens.

INTRODUCTION

A fingerprint is made of a series of ridges and furrows on the surface of the finger. The uniqueness of a fingerprint can be determined by the pattern of ridges and furrows as well as the minutiae points. Minutia consists of short ridges, Ridge ending and Bifurcation.

Fingerprint representations are based on the entire image, finger ridges, pores on the ridges, or salient features derived from the ridges. Representations predominantly based on ridge endings or bifurcations collectively known as minutiae.

Fingerprint matching techniques can be placed into two categories minutiae-based and correlation based. Minutiae-based techniques first find minutiae points and then map their relative placement on the finger. Correlation-based techniques require the precise location of a registration point and are affected by image translation and rotation.

Real and spoof fingerprints exhibit different textural characteristics based on structural, orientation roughness, smoothness and regularity differences of diverse regions in a fingerprint image.

TYPES OF FINGERPRINT PATTERNS

There are three main fingerprint patterns.

- Arches
- Loops
- Whorls

Arches are the ridges run from one side to the other of the pattern, making no backward turn. Plain arch is that type of pattern in which the ridges enter upon one side and make a rise or wave in the center as given in the Fig 1(a).

Tented arch is that type of pattern which possesses an angle, an up thrust, or two of the three basic characteristics of the loop as given in the Fig 1(b).

K. Anita Davamani*, Department of Computer Science & Engineering, BIST, BIHER, Chennai, TN, India.
E-mail: anitadavamani@gmail.com
S. Amudha, Department of Computer Science & Engineering, BIST, BIHER, Chennai, TN, India.
E-mail: amudha17s@gmail.com

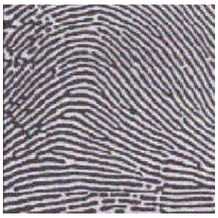

Fig. 1(a): Plain Arch

Fig. 1(b): Tented Arch

Loop is the type of pattern in which one or more ridges enter upon either side, recurve, touch or pass an imaginary line between delta and core and pass out or tend to pass out upon the same side the ridges entered. Loops which flow in the direction of the ulna bone (toward the little finger) are called ulnar loops as given in the Fig 2(a) and those which flow in the direction of the radius bone are called radial loops as given in the Fig 2(b).

Fig. 2(a): Radial

Fig. 2(b): Ulnar Loop

Whorl is a type of spiral or circular pattern. Plain whorl consists of one or more ridges which make or tend to make a complete circuit, with two deltas, between which, when an imaginary line is drawn, at least one recurving ridge within the inner pattern area is cut or touched as given in the Fig 3(a).Central pocket loop whorl consists of at least one recurving ridge, or an obstruction at right angles to the line of flow, with two deltas, between which, when an imaginary line is drawn, no recurving ridge within the inner pattern is cut or touched as given in the Fig 3(b).Double loop whorl consists of two separate loop formations, with Two separate and distinct sets of shoulders and two deltas as given in the Fig 3(c). Accidental whorl consists of a combination of two different types of patterns with the exception of the plain arch, with two or more deltas, or a pattern which possesses some of the requirements for two or more different types or a pattern which conforms to none of the definitions as given in the Fig 3(d).

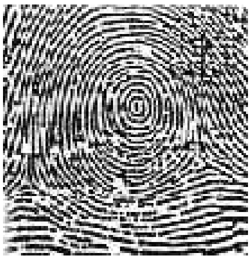

Fig. 3(a): Plain Whorl

Fig. 3(b): Central pocket loop whorl

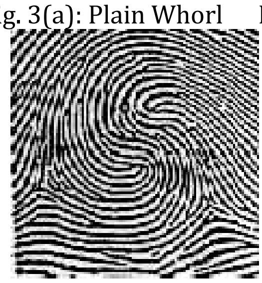

Fig. 3(c): Double Loop Whorl

Fig. 3(d): Accidental Whorl

RELATED WORKS

Liao.S et al.[1] paper comprises of two sets of features: dominant local Binary patterns (DLBP) in a texture image and the supplementary features extracted by using the circularly symmetric Gabor filter responses.It classifies the image texture using the Dominant Local Binary Pattern (DLBP) in which 80% of the most frequently occurred patterns are selected as features after the construction of Histogram. The DLBP approachon one side guarantees to be able to represent the dominant patterns in the texture images. On the other side, it retains the rotation invariant and histogram equalization invariant properties of the conventional LBP approach.

Regarding the selection of the first 80% most frequently appeared patterns as features after the pattern frequency histogram is constructed and sorted. It is experimentally shown that it gives good texture classification results. The global features extracted by using the circularly symmetric Gabor filter responses encapsulate the spatial relationships between distant pixels. The global features extracted from Gabor filter responses are Rotation invariant and less sensitive to histogram equalization. They, therefore, complement with the DLBP local features as mirrored by the experimental results.

Shankar Bhausaheb Nikam et al. [2] paper describes an image-based system to detect spoof fingerprint attacks in fingerprint biometric systems. It is based on the observation that, real and spoof fingerprints exhibit different textural characteristics. These are based on structural, orientation, roughness, smoothness and regularity differences of diverse regions in a fingerprint image. Local binary pattern (LBP) histograms are used to extract spatial gray level details.Ridge frequency and orientation details are exploited by decomposing a fingerprint in various approximation and detail sub bands using different wavelet filters. Textural characteristics are analyzed using LBP Histogram method and wavelet-based multiresolution analysis techniques.

Timo Ojala, Matti Pietikainen et al.[3] paper presents a theoretically efficient, multiresolution approach to gray-scale and rotation invariant texture classification based on local binary patterns. The method is based on recognizing that certain local binary patterns, termed uniform, are fundamental properties of local image texture and their occurrence histogram is proven to be a very powerful texture feature. Generalized gray scale and rotation invariant operator is derived for detecting the uniform patterns for any spatial resolution and presents a method for combining multiple operators for multiresolution analysis.

Arof.H et al.[4] paper introduces a texture descriptor that utilises circular neighborhoods and 1-D discrete Fourier transforms to obtain Rotation-invariant features. Since rotating an image does not change the intensities of its pixels but shifts them circularly, rotation invariant features can be realized if the relationship between circular motion and spatial shift is established. For each individual circular neighborhood centered at every pixel, a number of input sequences are formed by the intensities of pixels on concentric rings of various radii measured from the centre of each neighborhood. Fourier transforming the sequences would generate coefficients whose magnitudes are invariant to rotation. Features extracted from these magnitudes were used in various classification and segmentation experiments.

PROPOSED SYSTEM

The Dominant Local Binary Pattern (DLBP) method makes use of the most frequently occurred patterns. The DLBP approach computes the occurrence frequencies of all patterns defined in the LBP groups. These patterns are then sorted in ascending order. The first several most frequently occurring patterns should contain dominating patterns in the image i.e. it selects only the 80% of the total pattern occurrences in an image. These patterns effectively capture the image textural information for classification task.

PREPROCESSING

Preprocessing is a technique in which the data from an image are digitized and various mathematical operations are applied to the data, generally with a digital computer, in order to create an enhanced image that is more useful or to perform some of the interpretation and recognition task. Here Preprocessing technique is used for noise reduction of the Fingerprint image. Gabor Filter is used for noise reduction.

Gabor filter is a linear band pass filter and it is used for noise reduction. Gabor function is efficient for calculating the orientation feature. The Gabor filter represents the important properties of the fingerprint image as a pixel map. These include

1. <u>Orientation image</u>: The orientation image O represents the instantaneous ridge orientation at every point in the fingerprint image. The ridge orientation is not defined in regions where the ridges are not present.
2. <u>Frequency image</u>: The local ridge frequency indicates the average inter ridge distance within a block. Similar to the orientation image, the ridge frequency is not defined for background regions.
3. <u>Region mask</u>: The region mask indicates the parts of the image where ridge structures are present. It is also known as the foreground mask.

Some techniques are also able to distinguish between recoverable and unrecoverable regions.

The fingerprint image may be thought of as a system of oriented texture with non-stationary properties. Therefore traditional Fourier analysis is not adequate to analyze the image completely. We need to resolve the properties of the image both in space and also in frequency. We can extend the traditional one dimensional time-frequency analysis to two-dimensional image signals to perform short (time/space)-frequency analysis. When analyzing a non-stationary 1D signal $x(t)$ it is assumed that it is approximately stationary in the span of a temporal window $w(t)$ with finite support. The STFT of $x(t)$ is now represented by

Time frequency *atoms* $X(\tau,\omega)$ and is given by

$$X(\tau,w)=\int_{-\infty}^{\infty} x(t)w^*(t-\tau)\, e^{-jwt}dt \quad (1)$$

In the case of 2D signals such as a fingerprint image, the space-frequency *atoms* is given by

Here $\tau1$, $\tau2$ represent the spatial position of the two dimensional window W (x, y). $\omega1$, $\omega2$ represents the spatial frequency parameters. At each position of the window, it overlaps OVRLP pixels with the previous position. This preserves the ridge continuity and eliminates 'block' effects common with other block processing image operations. Each such analysis frame yields a single value of the dominant orientation and frequency in the region centered around ($\tau1$, $\tau2$).

Unlike regular Fourier transform, the result of the STFT is dependent on the choice of the window $w(t)$. For the sake of analysis any smooth spectral window such as hanning, hamming or even a Gaussian window may be utilized. However, since we are also interested in enhancing and reconstructing the fingerprint image directly from the Fourier domain, our choice of window is fairly restricted. In order to provide suitable reconstruction during enhancement, we utilize a raised cosine window that tapers smoothly near the border and is unity at the center of the window. The raised cosine spectral window is obtained using

$$W(x,y) = 1 \text{ if } (x,y) < BLKSZ/2 \text{ or } \tfrac{1}{2}(1+\cos(\pi x/OVRLP)) \quad (2)$$

Fourier spectrum of the real fingerprint images is characterized by a distribution of energies across all frequencies and orientations. We assume that the orientation θ is a random variable that has the probability density function $p(\theta)$. The expected value of the orientation may then be obtained by performing a vector averaging according to Equation below. The terms sin (2θ) and cos(2θ) are used to resolve the orientation ambiguity as mentioned before.

$$E\{\theta\} = \tfrac{1}{2}\tan^{-1}\{ \int_{\theta} p(\theta)\sin(2\theta)\, d\theta / \int_{\theta} p(\theta)\cos(2\theta)\, d\theta \quad (3)$$

The estimate is also optimal from a statistical sense. However, if there is a crease in the fingerprints that spans several analysis frames, the orientation estimation will still be wrong. The estimate will also be inaccurate when the frame consists entirely of unrecoverable regions with poor ridge structure or poor ridge contrast. In such instances, we can estimate the ridge orientation by considering the orientation of its immediate neighborhood.

The resulting orientation image *O(x,y)* is further smoothened using vectorial averaging. The smoothened image *O'(x,y)* is obtained using

$$O'(x,y)=1/2\ \{\tan^{-1} (\sin(2O(x,y))*W(x,y)/\cos(2O(x,y))*W(x,y))\} \quad (4)$$

Here W(x,y) represent a Gaussian smoothening kernel. Then inverse Fourier transform is applied to reconstruct the image. We perform an objective evaluation of the enhancement algorithm by considering the improvement in matching accuracy for poor quality prints.

Local Binary Pattern

The local binary pattern (LBP) operator was developed as a gray-scale invariant pattern measure adding complementary information to the “amount” of texture in images. It was first mentioned by Harwood et al. (1993), and introduced to the public by Ojala et al. (1996). Later, it has shown excellent performance in many comparative studies, in terms of both speed and discrimination performance. In a way, the approach is bringing together the separate statistical and structural approaches to texture analysis, opening a door for the analysis of both stochastic micro textures and deterministic macro textures simultaneously. It also seems to have some correspondence with new psycho physical findings in the human visual system. Furthermore, being independent of any monotonic transformation of grayscale, the operator is perfectly suited for complementing colour measurements or to be complemented by an orthogonal measure of image contrast. The LBP operator can be made invariant against rotation, and it also supports multi-scale analysis.

LBP is made invariant against the rotation of the image domain, and supplemented with a rotation invariant measure of local contrast. The LBP is proposed as a unifying texture model that describes the formation of a texture with micro-textons and their statistical placement rules.

The basic LBP is extended to facilitate the analysis of textures with multiple scales by combining neighbourhoods with different sizes.The local binary pattern (LBP) texture analysis operator is defined as a gray-scale invariant texture measure, derived from a general definition of texture in a local neighborhood. The basic idea is that a binary code that describes the local texture pattern is built by thresholding a neighborhood by the gray value of its center. The LBP feature vector, in its simplest form, is created in the following manner:

- Divide the examined window to cells (e.g. 16x16 pixels for each cell).
- For each pixel in a cell, compare the pixel to each of its 8 neighbors (on its left-top, left-middle, left-bottom, right-top, etc.). Follow the pixels along a circle, i.e. clockwise or counter-clockwise.
- Where the center pixel's value is greater than the neighbor, write "1". Otherwise, write "0". This gives an 8-digit binary number (which is usually converted to decimal for convenience).
- Compute the histogram, over the cell, of the frequency of each "number" occurring (i.e., each combination of which pixels are smaller and which are greater than the center).
- Optionally normalize the histogram.
- Concatenate normalized histograms of all cells.

This gives the feature vector for the window. An example is shown in Fig 4.

5	4	3
4	3	1
2	0	3

1	1	1
0		0
0	0	1

1	2	4
8		16
32	64	128

Fig. 4: LBP Code

LBP code= 1+2+4+0+0+0+0+128 = 135

Histogram is drawn for each LBP code as shown in Fig 5 found in each block based on its frequency.

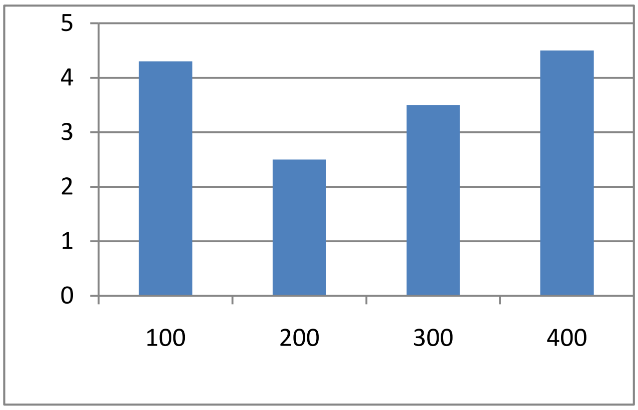

Fig. 5: LBP Histogram

DOMINANT LOCAL BINARY PATTERN: The conventional LBP approach is extended to the dominant local binary pattern (DLBP) approach in order to effectively capture the dominating patterns in texture images. Unlike the conventional LBP approach, which only exploits the uniform LBP, given a texture image, the DLBP approach computes the occurrence frequencies of all rotation invariant patterns defined in the LBP groups. These patterns are then sorted in ascending order as shown in Fig 6.

The first several most frequently occurring patterns should contain dominating patterns in the image and, therefore, are the dominant patterns. It is shown that the DLBP.

Approach is more reliable to represent the dominating pattern information in the texture images.

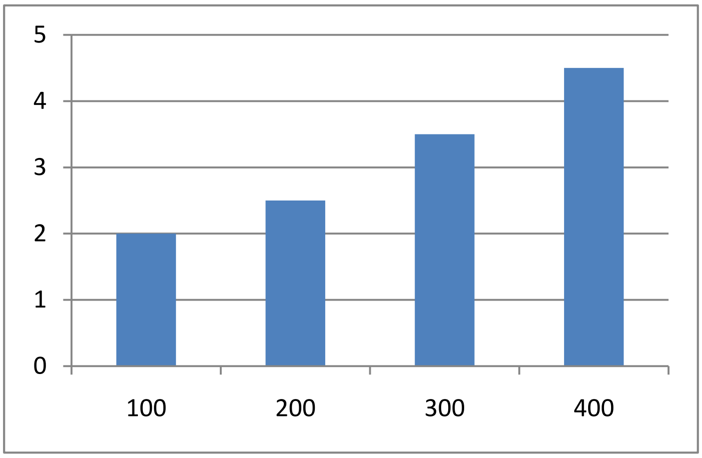

These Dominant patterns are then given to classification.In the conventional LBP method proposed by Ojala *et al*, only the uniform LBPs are considered. At a pixel, it gives a uniform LBP if the corresponding binary label sequence has no more than two transitions between "0" and"1" among all pairs of the adjacent binary labels.

For example, the binary label sequences "10001111" and "00011000" are uniform LBPs. But the sequence "01001111" is not a uniform LBP because it has four transitions. In the textures which mostly consist of straight edges or low curvature edges, the uniform LBPs effectively capture the fundamental information of textures. However, in practice, there are some texture images having more complicated shapes. These shapes can contain high curvature edges, crossing boundaries or corners. Performing texture classification on these textures based on uniform LBPs is possibly problematic.

The reason is that the uniform LBPs extracted from such images are not necessary to be the pattern shaving dominating proportions. Textural information cannot be effectively represented by solely considering the histogram of the uniform LBPs.

Although utilizing the uniform LBPs is insufficient to capture textural information, we avoid considering all the possible patterns to perform classification. As pointed out by Ojala *et al*, the occurrence frequencies of different patterns vary greatly and some of the patterns rarely occur in a texture image. The proportions of these patterns are too small and inadequate to provide a reliable estimation of the occurrence possibilities of these patterns.

Therefore, we propose to use dominant local binary patterns (DLBPs) which consider the most frequently occurred patterns in a texture image. It avoids the aforementioned problems encountered by merely using the uniform LBPs or making use of all the possible patterns, as the DLBPs are defined to be the most frequently occurred patterns. In this paper, it will be demonstrated that a minimum set of pattern labels that represents around 80% of the total pattern occurrences in an image can effectively captures the image textural information for classification tasks.

It is practically improbable to have two distinct texture types which can resemble dominant pattern proportions of each other. Without encapsulating the pattern type information, the DLBP features also possess surpassing robustness against image noise, as compared to the conventional LBP features. Under the effect of image noise, the binary label of a neighbouring pixel is possible to be flipped by the intensity distortion induced by noise. Flipped binary labels alter the extracted LBPs.

As a result, even though some LBPs are computed on the same type of image structures, the extracted LBP type can vary significantly. Thus, the pattern type information is unreliable. In the conventional LBP framework, the pattern types are categorized as uniform patterns or non uniform patterns. In which, under the effect of image noise, a large amount of useful patterns turns into non uniform ones that are unconsidered in the conventional LBP method. On the contrary, the DLBP approach processes all 80% dominant patterns disregarding the pattern types.

SUPPORT VECTOR MACHINE

Support Vector Machine (SVM) was first heard in 1992, introduced by Boser, Guyon, and Vapnik in COLT-92. Support vector machines (SVMs) are a set of related supervised learning methods used for classification and regression. They belong to a family of generalized linear classifiers. In another terms, Support Vector Machine (SVM) is a classification and regression prediction tool that uses machine learning theory to maximize predictive accuracy while automatically avoiding over-fit to the data. Support Vector machines can be defined as systems which use hypothesis space of a linear functions in a high dimensional feature space, trained with a learning algorithm from optimization theory that implements a learning bias derived from statistical learning theory.

Statistical Learning Theory

The statistical learning theory provides a framework for studying the problem of gaining knowledge, making predictions, making decisions from a set of data. In simple terms, it enables the choosing of the hyper plane space such a way that it closely represents the underlying function in the target space.

In statistical learning theory the problem of supervised learning is formulated as follows. We are given a set of training data $\{(x_1,y_1)... (x_l,y_l)\}$ in $R^n \times R$ sampled according to unknown probability distribution $P(x,y)$, and a loss function $V(y,f(x))$ that measures the error, for a given x, f(x) is "predicted" instead of the actual value y. The problem consists in finding a function f that minimizes the expectation of the error on new data that is, finding a function f that minimizes the expected error: $\int V(y,f(\mathbf{x}))\, P(\mathbf{x},y)\, d\mathbf{x}\, dy$

In statistical modeling we would choose a model from the hypothesis space, which is closest (with respect to some error measure) to the underlying function in the target space. More on statistical learning theory can be found on introduction to statistical learning theory.

There are many linear classifiers (hyper planes) that separate the data. However only one of these achieves maximum separation. The reason we need it is because if we use a hyper plane to classify, it might end up closer to one set of datasets compared to others and we do not want this to happen and thus we see that the concept of maximum margin classifier or hyper plane as an apparent solution. The equation of the hyper plane is given by

$$\boxed{\boldsymbol{W.X + b = 0}}$$

In this equation x is a vector point and w is weight and is also a vector. So to separate the data [a] should always be greater than zero. Among all possible hyper planes, SVM selects the one where the distance of hyper plane is as large as possible as shown in Fig 4.5. If the training data is good and every test vector is located in radius r from training vector. Now if the chosen hyper plane is located at the farthest possible from the data. This desired hyper plane which maximizes the margin also bisects the lines between closest points on convex hull of the two datasets.

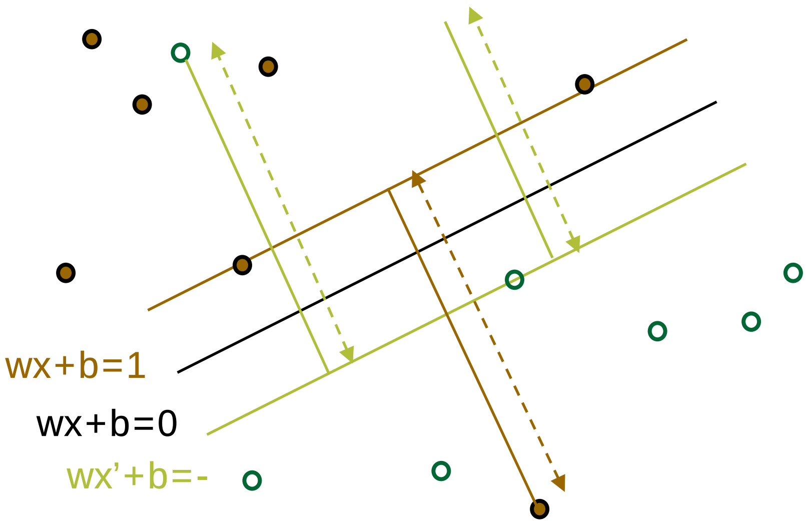

Fig. 6: Representation of Hyper planes

Distance of closest point on hyper plane to origin can be found by maximizing the x as x is on the hyper plane. Similarly for the other side points we have a similar scenario. Thus solving and subtracting the two distances we get the summed distance from the separating hyper plane to nearest points.

$$\boxed{M = 2 / ||w||}$$

SVM for Classification

SVM is a useful technique for data classification. Even though it's considered that Neural Networks are easier to use than this, however, sometimes unsatisfactory results are obtained. A classification task usually involves with training and testing data which consist of some data instances. Each instance in the training set contains one target values and several attributes.

The goal of SVM is to produce a model which predicts target value of data instances in the testing set which are given only the attributes. Classification in SVM is an example of Supervised Learning. Known labels help indicate whether the system is performing in a right way or not.

This information points to a desired response, validating the accuracy of the system, or be used to help the system learn to act correctly. A step in SVM classification involves identification as which are intimately connected to the known classes. This is called feature selection or feature extraction. Feature selection and SVM classification together have a use even when prediction of unknown samples is not necessary. They can be used to identify key sets which are involved in whatever processes distinguish the classes.

Kernel: If data is linear, a separating hyper plane may be used to divide the data. However it is often the case that the data is far from linear and the datasets are inseparable. To allow for this kernels are used to non-linearly map the input data to a high-dimensional space. The new mapping is then linearly separable. A very simple illustration of this is shown below in Fig 7.

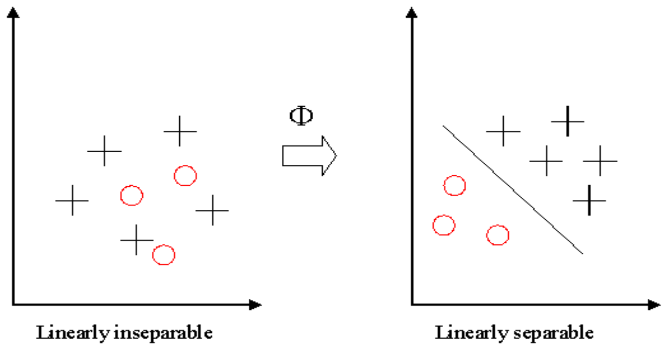

Support Vector Machines acts as one of the best approach to data modeling. They combine generalization control as a technique to control dimensionality. The kernel mapping provides a common base for most of the commonly employed model architectures, enabling comparisons to be performed. In classification problems generalization control is obtained by maximizing the margin, which corresponds to minimization of the weight vector in a canonical framework. The solution is obtained as a set of support vectors that can be sparse. The minimization of the weight vector can be used as a criterion in regression problems, with a modified loss function.

CONCLUSION

Dominant patterns retain the rotation invariant and histogram equalization invariant properties of the conventional LBP approach. Regarding the selection of the first 80% most frequently appeared patterns as features after the pattern frequency histogram is constructed and sorted. The Output is validated on real fingerprint datasets and classification is found to be efficient which shows the error rate as 0.4%.

FUTURE WORK

For further improvisation of the accurate classification of the texture, better optimization techniques such as Genetic algorithms can be used. This would help in improving accuracy in classification for much efficiency.

REFERENCES

[1] Das, J., Das, M. P., & Velusamy, P. (2013). Sesbania grandiflora leaf extract mediated green synthesis of antibacterial silver nanoparticles against selected human pathogens. *Spectrochimica Acta Part A: Molecular and Biomolecular Spectroscopy*, *104*, 265-270.

[2] Umanath, K.P.S.S.K., Palanikumar, K., & Selvamani, S. T. (2013). Analysis of dry sliding wear behaviour of Al6061/SiC/Al2O3 hybrid metal matrix composites. *Composites Part B: Engineering*, *53*, 159-168.

[3] Udayakumar, R., Khanaa, V., Saravanan, T., & Saritha, G. (1786). Cross layer optimization for wireless network (WIMAX). *Middle-East Journal of Scientific Research*, *16*(12), 1786-1789.

[4] Kumaravel, A., & Rangarajan, K. (2013). Algorithm for automaton specification for exploring dynamic labyrinths. *Indian Journal of Science and Technology*, *6*(5S), 4554-4559.

[5] Pieger, S., Salman, A., & Bidra, A.S. (2014). Clinical outcomes of lithium disilicate single crowns and partial fixed dental prostheses: a systematic review. *The Journal of prosthetic dentistry*, *112*(1), 22-30.

[6] Vijayaraghavan, K., Nalini, S.K., Prakash, N.U., & Madhankumar, D. (2012). One step green synthesis of silver nano/microparticles using extracts of Trachyspermum ammi and Papaver somniferum. *Colloids and Surfaces B: Biointerfaces*, *94*, 114-117.

[7] Khanaa, V., Mohanta, K., & Satheesh, B. (2013). Comparative study of uwb communications over fiber using direct and external modulations. *Indian Journal of Science and Technology*, *6*(6), 4845-4847.

[8] Khanaa, V., Thooyamani, K. P., & Udayakumar, R. (1798). Cognitive radio based network for ISM band real time embedded system. *Middle-East Journal of Scientific Research*, *16*(12), 1798-1800.

[9] Vijayaraghavan, K., Nalini, S.K., Prakash, N.U., & Madhankumar, D. (2012). Biomimetic synthesis of silver nanoparticles by aqueous extract of Syzygium aromaticum. *Materials Letters*, *75*, 33-35

[10] Caroline, M.L., Sankar, R., Indirani, R.M., & Vasudevan, S. (2009). Growth, optical, thermal and dielectric studies of an amino acid organic nonlinear optical material: l-Alanine. *Materials Chemistry and Physics*, *114*(1), 490-494.

[11] Kumaravel, A., & Pradeepa, R. (2013). Efficient molecule reduction for drug design by intelligent search methods. *International Journal of Pharma and Bio Sciences*, *4*(2), B1023-B1029.

[12] Kaviyarasu, K., Manikandan, E., Kennedy, J., Jayachandran, M., Ladchumananandasiivam, R., De Gomes, U. U., & Maaza, M. (2016). Synthesis and characterization studies of NiO nanorods for enhancing solar cell efficiency using photon upconversion materials. *Ceramics International*, *42*(7), 8385-8394.

[13] Sengottuvel, P., Satishkumar, S., & Dinakaran, D. (2013). Optimization of multiple characteristics of EDM parameters based on desirability approach and fuzzy modeling. *Procedia Engineering*, *64*, 1069-1078.

[14] Anbuselvi S., Chellaram, C., Jonesh S., Jayanthi L., & Edward J.K.P. (2009). Bioactive potential of coral associated gastropod, Trochus tentorium of Gulf of Mannar, Southeastern India. *J. Med. Sci,* 9(5), 240-244.

[15] Kaviyarasu, K., Ayeshamariam, A., Manikandan, E., Kennedy, J., Ladchumananandasivam, R., Gomes, U. U., & Maaza, M. (2016). Solution processing of CuSe quantum dots: Photocatalytic activity under RhB for UV and visible-light solar irradiation. *Materials Science and Engineering: B*, *210*, 1-9.

[16] Venkatesh Guru, K. (2015). Active Low Energy Outlay Routing Algorithm for Wireless Ad Hoc Network. *International Journal of Communication and Computer Technologies, 3*(1), 6-8.

[17] Surendheran, A.R., & Prashanth, K. (2015). A Survey of Energy-Efficient Communication Protocol for Wireless Sensor Networks. *International Journal of Communication and Computer Technologies, 3*(2), 50-57.

[18] Han, D.H., & Nv, Z. (2017). Mining Frequent Patterns in Large Scale Databases Using Adaptive FP-Growth Approach. *Bonfring International Journal of Industrial Engineering and Management Science, 7*(2), 17-20.

[19] Zahedifard, M., & Attarzadeh, I., Pazhokhzadeh, H., & Malekzadeh, J. (2015). Prediction of students' performance in high school by data mining classification techniques. *International Academic Journal of Science and Engineering, 2*(7), 25-33.

[20] Poursheikhi, M., & Torkestanib, J.A. (2015). To present the new structure to better manage and control requests in the national information network based SDN architecture. *International Academic Journal of Science and Engineering, 2*(7), 34-50.

[21] Suganya, M., Bramanayaki, S., Sri Nandhini, S., & Subbulakshmi, P. (2014). Locating Center of Optic Disc in Retinal Images. *International Journal of System Design and Information Processing, 2*(3), 54-58.

[22] Sivaranjani, S. (2018). Detecting Congestion Patterns in Spatio Temporal Traffic Data Using Frequent Pattern Mining. *Bonfring International Journal of Networking Technologies and Applications, 5*(1), 21-23.

[23] Smith, J., and Sebastian, J. (2017). Feeder Automation and its Reliability Assessment on the Basis of Cost Analysis for the Distribution of Feeders in Power System Planning. *Bonfring International Journal of Power Systems and Integrated Circuits, 7*(2), 19-26.

[24] Balagopalan, S., Aravind, T., Sreehari, G.N., Praveesh, V.V., & Padmanabhan, G.G.N. (2014). E-waste Management Schools for the Homeless. *International Scientific Journal on Science Engineering & Technology, 17*(11), 1026-1032.

[25] Rajendra, M.A., & Puranik Vipin, G. (2014). Airbag Deployment System Based On Pre-crash Information. *International Scientific Journal on Science Engineering & Technology, 17*(10), 975-981.

[26] Kumaravel, A., & Udayakumar, R. (2013). Web portal visits patterns predicted by intuitionistic fuzzy approach. *Indian Journal of Science and Technology*, *6*(5S), 4549-4553.

[27] Srinivasan, V., & Saravanan, T. (2013). Reformation and market design of power sector. *Middle-East Journal of Scientific Research*, *16*(12), 1763-1767.

[28] Kaviyarasu, K., Manikandan, E., Kennedy, J., & Maaza, M. (2015). A comparative study on the morphological features of highly ordered MgO: AgO nanocube arrays prepared via a hydrothermal method. *RSC Advances*, *5*(100), 82421-82428.

[29] Kumaravel, A., & Udhayakumarapandian, D. (2013). Consruction of meta classifiers for apple scab infections. *International Journal of Pharma and Bio Sciences*, *4*(4), B1207-B1213.

[30] Sankari, S. L., Masthan, K. M. K., Babu, N. A., Bhattacharjee, T., & Elumalai, M. (2012). Apoptosis in cancer-an update. *Asian Pacific journal of cancer prevention*, *13*(10), 4873-4878

[31] Harish, B. N., & Menezes, G. A. (2011). Antimicrobial resistance in typhoidal salmonellae. *Indian journal of medical microbiology*, *29*(3), 223-229.

[32] Manikandan, A., Manikandan, E., Meenatchi, B., Vadivel, S., Jaganathan, S. K., Ladchumananandasivam, R., & Aanand, J. S. (2017). Rare earth element (REE) lanthanum doped zinc oxide (La: ZnO) nanomaterials: synthesis structural optical and antibacterial studies. *Journal of Alloys and Compounds*, *723*, 1155-1161.

[33] Caroline, M. L., & Vasudevan, S. (2008). Growth and characterization of an organic nonlinear optical material: L-alanine alaninium nitrate. *Materials Letters*, *62*(15), 2245-2248.

[34] Saravanan T., Srinivasan V., Udayakumar R. (2013). A approach for visualization of atherosclerosis in coronary artery, Middle - East Journal of Scientific Research, 18(12), 1713-1717.

[35] Poongothai, S., Ilavarasan, R., & Karrunakaran, C.M. (2010). Simultaneous and accurate determination of vitamins B1, B6, B12 and alpha-lipoic acid in multivitamin capsule by reverse-phase high performance liquid chromatographic method. *International Journal of Pharmacy and Pharmaceutical Sciences*, *2*(4), 133-139.

[36] Udayakumar, R., Khanaa, V., & Saravanan, T. (2013). Synthesis and structural characterization of thin films of SnO 2 prepared by spray pyrolysis technique. *Indian Journal of Science and Technology*, *6*(6), 4754-4757

[37] Anbazhagan, R., Satheesh, B., & Gopalakrishnan, K. (2013). Mathematical modeling and simulation of modern cars in the role of stability analysis. *Indian Journal of Science and Technology*, *6*(5S), 4633-4641.

[38] Caroline, M.L., & Vasudevan, S. (2009). Growth and characterization of bis thiourea cadmium iodide: A semiorganic single crystal. *Materials Chemistry and Physics*, *113*(2-3), 670-674.

[39] Sharmila, S., Jeyanthi Rebecca, L., & Das, M. P. (2012). Production of Biodiesel from Chaetomorpha antennina and Gracilaria corticata. *Journal of Chemical and Pharmaceutical Research*, *4*(11), 4870-4874.

[40] Thooyamani, K.P., Khanaa, V., & Udayakumar, R. (2013). An integrated agent system for e-mail coordination using jade. *Indian Journal of Science and Technology*, *6*(6), 4758-4761.

[41] Caroline, M. L., Kandasamy, A., Mohan, R., & Vasudevan, S. (2009). Growth and characterization of dichlorobis l-proline Zn (II): A semiorganic nonlinear optical single crystal. *Journal of Crystal Growth*, *311*(4), 1161-1165.

[42] Caroline, M.L., & Vasudevan, S. (2009). Growth and characterization of L-phenylalanine nitric acid, a new organic nonlinear optical material. *Materials Letters*, *63*(1), 41-44.

[43] Kaviyarasu, K., Xolile Fuku, Genene T. Mola, E. Manikandan, J. Kennedy, and M. Maaza. Photoluminescence of well-aligned ZnO doped CeO2 nanoplatelets by a solvothermal route. *Materials Letters*, *183*(2016), 351-354.

[44] Saravanan, T., & Saritha, G. (2013). Buck converter with a variable number of predictive current distributing method. *Indian Journal of Science and Technology*, *6*(5S), 4583-4588.

[45] Parthasarathy, R., Ilavarasan, R., & Karrunakaran, C. M. (2009). Antidiabetic activity of Thespesia Populnea bark and leaf extract against streptozotocin induced diabetic rats. *International Journal of PharmTech Research*, *1*(4), 1069-1072.

[46] Hanirex, D. K., & Kaliyamurthie, K. P. (2013). Multi-classification approach for detecting thyroid attacks. *International Journal of Pharma and Bio Sciences,* 4(3), B1246-B1251

[47] Kandasamy, A., Mohan, R., Lydia Caroline, M., & Vasudevan, S. (2008). Nucleation kinetics, growth, solubility and dielectric studies of L-proline cadmium chloride monohydrate semi organic nonlinear optical single crystal. *Crystal Research and Technology: Journal of Experimental and Industrial Crystallography*, *43*(2), 186-192.

[48] Srinivasan, V., Saravanan, T., Udayakumar, R., & Saritha, G. (2013). Specific absorption rate in the cell phone user's head. *Middle-East Journal of Scientific Research*, *16*(12), 1748-50.

[49] Udayakumar R., Khanaa V., & Saravanan T. (2013). Chromatic dispersion compensation in optical fiber communication system and its simulation, Indian Journal of Science and Technology, 6(6), 4762-4766.

[50] Vijayaragavan, S.P., Karthik, B., Kiran, T.V.U., & Sundar Raj, M. (1990). Robotic surveillance for patient care in hospitals. *Middle-East Journal of Scientific Research*, *16*(12), 1820-1824.